International Journal of Service and Knowledge Management
International Institute of Applied Informatics
2023, Vol. 7, No. 2, IJSKM770

Scenario Analysis of Demand Response Using Artificial Electric Power Market Simulations

Masanori Hirano *, Ryo Wakasugi *, Kiyoshi Izumi *

Abstract

We created and analyzed various Demand Response (DR) scenarios in the electric power market using multi-agent simulation. We first built a multi-agent simulation for the electric power market using actual data, including prices from the Japanese Electric Power Exchange (JEPX) market, electricity consumption in Japan, and an actual factory. Using this multi-agent simulation, we tested several possible DR scenarios for the factory. We then compared these scenarios using two newly defined indices for assessing the reduction efficiency of cost and CO_2 emissions. The results showed that a work time shift in the summer and peak shift in factory demand in the winter were the best in terms of cost and CO_2 emission reduction efficiencies. Thus, we demonstrated the usefulness of our multi-agent simulation for examining the effectiveness of DR scenarios by simulating complex interactions that consider the seasonal and time-of-day characteristics of power prices.

Keywords: decarbonization, demand response, electric power market, multi-agent simulation

1 Introduction

Climate change risk is now a major global issue, with many countries, organizations, and companies taking steps to prevent global warming. Individual companies are also increasingly expected to reduce CO_2 emissions, increasing the demand and requirement for CO_2 emission neutralization.

In addition, with the expansion of Environmental, Social, and Governance (ESG) investments, companies are beginning to take steps toward carbon neutrality to enhance value creation. Currently, achieving carbon neutrality is not easy and requires a combination of various measures, such as energy conservation, introducing renewable energy, and purchasing Renewable Energy Certificate (REC), Guarantee of Origin (GO), and International Renewable Energy Certificate (I-REC).

Meanwhile, in some countries and regions, electric power markets have been deregulated to decrease electricity prices and promote technological innovation. However, this deregulation can cause instability in the power grid and significant price fluctuations in grid

* The University of Tokyo, Tokyo, Japan

power. For example, after the gradual deregulation of the Japan Electric Power Exchange (JEPX) market in 2005, significant price fluctuations caused social disruption.

Moreover, challenges to carbon neutrality can increase the instability of these electric power markets much more. Renewable power sources, such as photovoltaics and wind turbines, are unstable owing to various factors, including the weather.

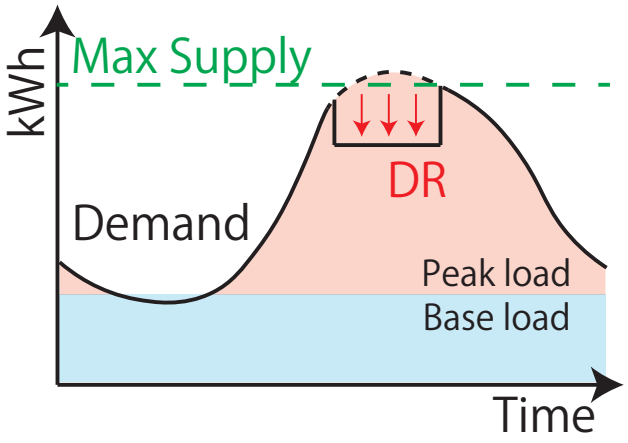

Figure 1: Concept of DR.

One possible solution to stabilize power prices is demand response (DR), which can also reduce CO_2 emissions and lower costs. DR is the change in the power consumption volume of consumers to reduce the peak demand in the power grid, and stabilize the balance between the power generation limit and consumption (See also Figure 1). It is primarily intended to reduce the peak load demand such that it does not exceed the total generation limit of the power grid. Thus, DR not only stabilizes the power grid, but also reduces CO_2 emissions of each consumer. In general, because electricity for the peak load is supplied by gas-fired power generation, which have a higher CO_2 emission factor. Therefore, reducing the peak load can help reduce CO_2 emissions. DR can also contribute to reducing the cost of electricity procurement because the peak load prices are relatively high.

In this study, we examined multiple DR scenarios for a factory using multi-agent simulation. The effects of DR can be estimated without such simulations; however, an accurate comparison of DR scenarios is difficult and the feasibility of each scenario is not guaranteed without market interaction. For example, a large-scale DR can cause market impacts (i.e., the effect of the trading on markets). In addition, if the same strategy is always used for DR, other market participants could plan the opposite strategy and exploit the DR effects. Thus, multi-agent simulation is a promising way to investigate DR scenarios and understand the indirect effects of complex interactions.

We focus on JEPX and one factory in a major Japanese electric industry company. This factory was modeled based on its data to investigate the impact of multiple DR scenarios on it.

2 Related Work

According to [1], electric power market have been gradually deregulated in many countries since the 1990s. Deregulation is assumed to enhance the price competition principle of markets [2] and is aimed at providing long-term benefits to consumers [1].

Meanwhile, climate change has become an important problem in the electric power market in terms of CO_2 emissions. The Intergovernmental Panel on Climate Change (IPCC) has noted that climate change is affecting the world, and limiting global warming to 2 °C – 1.5 °C is achievable and beneficial [3]. Therefore, reducing CO_2 emissions has become essential.

Under this situation, the stability of the electric power is a crucial problem for two reasons: First, a deregulated power market causes imbalances between demand and supply. Second, the output of decarbonized power sources, such as photovoltaic power generation, are unstable. DR is considered a promising approach to avoid these imbalances [4]. Thus, we focused on DR in this study.

To analyze the effect of DR on the electric power market, we need to consider the complex mutual effects because the prices are decided by the supply-demand balance, which is affected by all participants in the market. Therefore, a multi-agent simulation is a promising approach [5, 6]. Multi-agent simulations are used to simulate the interaction of all individuals (agents) and investigate the micro-macroscopic results of their interactions. These simulations have been also applied to the electric power market [7].

Sensfuss [8] proposed a multi-agent simulation-based platform for Germany called PowerACE, which includes a power supply, power demand, renewable energy generation, power market, and battery. Sensfuss *et al.* [9] analyzed the impact of the emergence of renewable energy on the German electric power market using PowerACE. Weiss *et al.* [10] used a multi-agent model to discuss the investment incentives for power generation plants in an electric power grid where all power sources are renewable. Ken *et al.* [11] analyzed the effect and design of feed-in premiums in Japan using an electric power market simulation.

Similarly, Chuang *et al.* [12] applied the Cournot model to a competitive electric power market to analyze the expansion of power generation and showed the advantages of a competitive market over a centralized one for the expansion. Day *et al.* [13] used the supply function equilibrium model where all players submit prices and the corresponding volumes to analyze the impact of the policy introduced in England and Wales to improve market efficiency. The authors argued for the need for continuous strict price monitoring and controls. Jiang *et al.* [14] proposed a game-theoretic pricing model for peer-to-peer (P2P) electricity trading in a blockchain for energy, showing that P2P electricity trading can be beneficial and contribute to the development of electric power markets. Ghaffari *et al.* [15] discussed models for tradeable green certificates based on game theory and concluded that the Stackelberg game model was the most appropriate. However, because these game theory-based analyses typically employ strong assumptions, it is difficult to consider the complex real-world situation of an electric power market [8].

Regarding DR studies, Kok *et al.* [16] proposed Power Matcher, a multi-agent framework, and showed that the flexibility of generation and consumption is important. In this framework, agents control electricity consumption and generating devices, and strategically publish their orders in the market. Oh *et al.* [17] utilized a multi-agent simulation to investigate the best bidding strategy and showed that DR could contribute to market efficiency. Zhou *et al.* [18] conducted simulation experiments on the DR of commercial buildings using a multi-agent model and investigated the effect of DR. However, these studies did not analyze DR for factories in terms of cost or CO_2 emissions, which we address in this study.

3 Simulation Model

The JEPX spot market (previous day trading) was used as the basis for the simulation model because it is the main market of JEPX. In the simulation, there are 48 markets for every 30 minutes of electricity usage with a blinded single-price batch auction mechanism, which is the same as the spot market. Some agents participate in these markets and place orders based on their power usage or generation plan. Such a simulation is commonly referred to as a "multi-agent simulation." We regarded one step as one day and all experiments completed 365 steps.

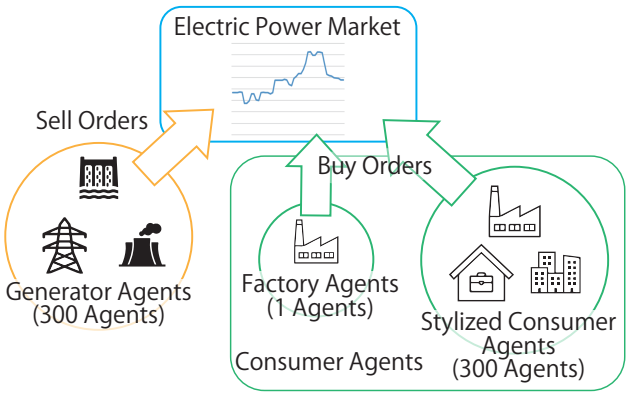

Figure 2: Simulation Model Outline

An overview of this simulation is shown in Figure 2. As described below, one type of generator agent and two types of consumer agents constitute the simulation. Each agent has a plan regarding the use or generation of electricity, and a strategy regarding the procurement or supply of electricity. The simulation behaves like a real electric power market by aggregating the actions of these agents.

3.1 Generator Agent

We employed 300 generator agents that supply power to the electric grid. Each agent has a hydroelectric, nuclear, petroleum thermal, gas-fired thermal, and coal-fired thermal power plant. The agents then determined their limit sell orders based on the unit power prices of those power sources, as described below.

3.1.1 Power Supply Configuration and Unit Cost

First, a total supply configuration of 300 agents was set based on the actual power supply configuration in Japan [1]. The configuration is listed in Table 1. Based on the power supply configuration, each type of power generation volume is randomly allocated to 300 agents (by scaling 300 random variables generated from a uniform distribution). Based on each power supply configuration, agents' configurations and unit costs of power generation are determined using the unit cost of each power generation method for the agents. The unit power generation costs are calculated using actual data from Japan [2].

[1] https://www.enecho.meti.go.jp/statistics/total_energy/results.html

[2] https://www.enecho.meti.go.jp/committee/council/basic_policy_subcommittee/index.html

Table 1: Power supply configuration in the entire power market

Hydroelectric	Nuclear	Thermal		
		Petroleum	Gas-fired	Coal-fired
8.8%	6.6%	7.7%	41.8%	35.2%

3.1.2 Offering (Selling) Price

At the kth ($k \in \{0,\cdots,47\}$) market on day $t(\in \{0,\cdots,364\})$, agent i's offering price $\hat{p}_t^{k,i,s}$ for the power supply method s is determined as follows:

$$\hat{p}_t^{k,i,s} = p_{t-1}^k \exp\left(\hat{r}_t^{k,i,s}\right), \tag{1}$$

$$\hat{r}_t^{k,i,s} = \frac{w_B^i B_t^{k,i,s} + w_C^i C_t^{k,i,s} + w_N^i N_t^{k,i,s}}{w_B^i + w_C^i + w_N^i}, \tag{2}$$

where p_{t-1}^k is the previous day's market price in the kth market, and w_B^i, w_C^i, and w_N^i are the random weights for the base $B_t^{k,i,s}$, technical (chart) $C_t^{k,i,s}$, and noise terms $N_t^{k,i,s}$, respectively. w_B^i, w_C^i, and w_N^i are generated from the uniform distributions $[0, W_B^g], [0, W_C^g]$, and $[0, W_N^g]$, respectively. W_B^g is set to 1.0 and W_C^g, W_N^g are set via a parameter grid search to obtain realistic results (see Section 5). Each term is calculated as follows:

$$B_t^{k,i,s} = \frac{g_t^s}{\varepsilon^{i,s}}(1 + r^{i,s}), \tag{3}$$

$$C_t^{k,i,s} = \frac{1}{\tau}\sum_{l=1}^{\tau} \ln \frac{p_{t-l}^k}{p_{t-l-1}^k}, \tag{4}$$

$$N_t^{k,i,s} \sim \mathcal{N}(0,1), \tag{5}$$

where g_t^s is the previously mentioned unit cost for power generation method s on day t, $\varepsilon^{i,s}$ is the power generation efficiency variable from a uniform distribution $[0.8, 1.2]$, $r^{i,s}$ is agent i's additional profit ratio for the generation method s from the uniform distribution $[0.0, 0.2]$, τ is a technical analysis window set to seven, and $\mathcal{N}(0,1)$ represents a standard normal distribution. These refer to [19]. Through these calculations that imitate actual decision-making scenarios, agents have heterogeneity and make the market more realistic with merit orders (the lower order of the marginal cost of each power generation).

3.1.3 Offering (Selling) Volume

Agent i's electric power offering volume for the power generation method s in the k th market on day t is calculated as follows:

$$q_t^{k,i,s} = \overline{q}_t^{k,i,s} + \Delta q_t^{k,i,s}, \tag{6}$$

where $\overline{q}_t^{k,i,s}$ and $\Delta q_t^{k,i,s}$ are the reference and controlled power generation volumes, respectively. Because base-load power plants cannot control their power output instantaneously, $\Delta q_t^{k,i,s}$ is set to 0 for hydroelectric and nuclear power plants. By contrast, thermal plants can

easily control their supply. Thus, we assume that thermal plants control their power generation volume according to the predicted demand based on the previous week's demand, as given below.

$$\Delta q_t^{k,i,s} = \eta_i \frac{(D_{t-7}^k - S_{t-7}^k) q_{t-7}^{k,i}}{S_{t-7}^k} \lambda_t^{k,i,s}, \tag{7}$$

where D_{t-7}^k and S_{t-7}^k represent the total demand and supply in the kth market on the same day in the previous week, respectively. $q_{t-7}^{k,i}$ is agent i's total supply in the market, η_i is agent i's responsiveness to the supply-demand imbalance obtained from a uniform distribution $[0.5, 2.0]$, and $\lambda_t^{k,i,s}$ represents the share of the power generation method s in the total controllable power generation volume of agent i.

3.2 Stylized Consumer Agent

The stylized consumer agent is the only type of consumer agent, except for one factory agent. The demands of this type of agent are predefined and only their bidding prices change.

Agent j's bidding price in the kth market on day t is calculated as follows:

$$\hat{p}_t^{k,j} = p_{t-1}^k \exp(\hat{r}_t^{k,j}), \tag{8}$$

$$\hat{r}_t^{k,j} = \frac{w_F^j F_t^{k,j} + w_C^j C_t^{k,j} + w_N^j N_t^{k,j}}{w_F^j + w_C^j + w_N^j}, \tag{9}$$

where w_F^j, w_C^j, and w_N^j are the random weights for the fundamental $F_t^{k,j}$, technical (chart) $C_t^{k,j}$, and noise terms $N_t^{k,j}$, respectively. w_F^j, w_C^j, and w_N^j are generated from the uniform distributions $[0, W_F^d], [0, W_C^d], and [0, W_N^d]$, respectively. W_F^d is set to 1.0, and W_C^d and W_N^d are set via a parameter grid search to obtain realistic results (see Section 5). Each term is calculated as follows:

$$F_t^{k,j} = \ln \frac{p_F^*}{p_{t-1}^k} \tag{10}$$

$$C_t^{k,j} = \frac{1}{\tau} \sum_{l=1}^{\tau} \ln \frac{p_{t-l}^k}{p_{t-l-1}^k}, \tag{11}$$

$$N_t^{k,j} \sim \mathcal{N}(0,1), \tag{12}$$

where p_F^* is the theoretical fundamental price and is set to 10; the other notations are the same as those of the generator agents. These are also based on [19].

The bidding volume is set externally based on actual Japanese demand data[3]. We distribute the actual consumption volume among the 300 agents in the market for each period.

3.3 Factory Agent

The agent's behavior is modeled to mimic actual factory demand patterns. To replicate the actual demand pattern, demand was modeled based on the principal component analysis (PCA) of the actual data. Then, according to the modeled demand, this agent issues orders whose prices are assumed to be sufficiently high for execution. The details are as follows.

[3] `https://www.tepco.co.jp/forecast/html/area_data-j.html`;
`https://powergrid.chuden.co.jp/denkiyoho/`;
`https://www.kansai-td.co.jp/denkiyoho/area-performance.html`

3.3.1 PCA and Demand Modeling

We found two major components for actual factory power usage according to our PCA analysis:

- First principal component (68.7%): This component contributes 68.7% and is significant only in the daytime on a weekday. Thus, we regarded it as the base demand of production activities.
- Second principal component (9.1%): This component contributes 9.1%, and is more significant in summer and winter than in spring and autumn. Thus, we regarded it as a seasonal factor, including air conditioners (AC).
- Other components (22.2%): The remaining 22.2%, which cannot be explained by the first and second components, was regarded as noise factors.

Based on these components, we modeled the demand for this factory as follows:

$$d_t^{k,\star} = w_B^\star B_t^{k,\star} + w_A^\star A_t^{k,\star} + w_N^\star N_t^{k,\star}, \tag{13}$$

where $B_t^{k,\star}$, $A_t^{k,\star}$, and $N_t^{k,\star}$ are the base, AC, and noise factors, respectively, which are modeled based on the aforementioned components, and $w_B^\star, w_A^\star$, and $w_N^\star$ are their respective weights. $w_B^\star$ and $w_A^\star$ are determined according to the actual demand, and $w_N^\star$ is set to 10% of the total demand. This is because the contribution of each component of the PCA does not mean the scale of each component. Finally, the factory's total demand share in the market is set to 2.26×10^{-6} based on the actual share.

3.3.2 DR

The demand for this factory agent is determined using Eq. 13; however, this demand can be modified by the DR scenarios. Each scenario is described in detail in section 4.

3.3.3 Bidding

After considering DR, the factory agent places buy orders at a sufficiently high price because the market employs a blind single-price batch auction with only one execution price. Therefore, to obtain sufficient power, the agent needs to place an order at a sufficiently high price; the high bid price has no effect on the execution price.

4 DR Scenarios

We created two types of DR scenarios for factory agents: peak-cut (or peak shaving), and peak shift. Table 2 presents the summary of each scenario.

Table 2: List of DR Scenarios

Scenario Name	Type	DR Target	Target Market (Summer)	Target Market (Winter)
Fixed Cut	Peak-Cut	All possible machines + AC	12:00–15:00 (6 markets: 25th–30th)	17:00-20:00 (6 markets: 35th–40th)
Price-based Flexible Cut		All possible machines + AC	Automatically selected 6 markets (3 hours in total) in the working hours (9:00–17:00) based on price, CO_2 emissions, and demand of the same market in the previous week, respectively.	
CO_2 emissions-based Flexible Cut		All possible machines + AC		
Demand-based Flexible Cut		All possible machines + AC		
AC Shift		AC (Summer only)	Downward: 14:00–17:00 (29th–34th) Upward: 9:00–13:00 (19th–28th)	N/A
Work Time Shift	Peak Shift	Working hour	H hours ahead ($H = 0.5, 1.0, 1.5, 2.0, 2.5, 3.0$)	
Fixed Shift		All possible machines + AC	Downward: 12:00–15:00 Upward: Other between 9:00–17:00	Downward: 9:00–10:30; 15:30–17:00 Upward: Other between 9:00–17:00
Price-based Flexible Shift		All possible machines + AC	Automatically select 6 markets each (3 hours in total) in the working hours (9:00–17:00) for upward (demand increase) and downward (demand decrease) DR, respectively, based on price, CO_2 emissions, and demand of the same market in the previous week, respectively.	
CO_2 emissions-based Flexible Shift		All possible machines + AC		
Demand-based Flexible Shift		All possible machines + AC		

Price and CO_2 emissions per kWh are important for DR planning. We show them in the simulations, as illustrated in Figures 3 and 4. We only consider the summer and winter periods because the electric power supply is tight. In the simulation, steps 60–152 and 244–334 correspond to the summer (June – August) and winter seasons (December – February), respectively. From Figures 3 and 4, we can observe one peak in the summer and two peaks in the winter. Although these graphs are generated based on simulated data, the characteristics of these movements correspond to the actual movements. Based on these figures, the DR scenarios were set up as follows.

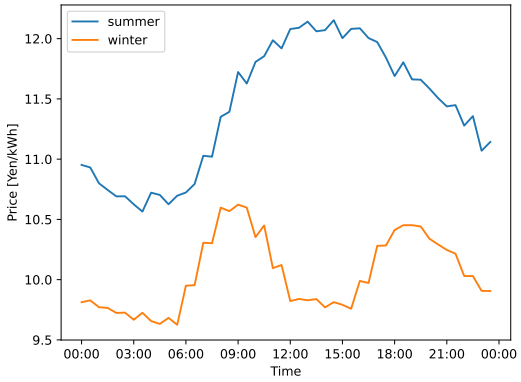

Figure 3: Price movement in the summer and winter (averaged of 100 simulations)

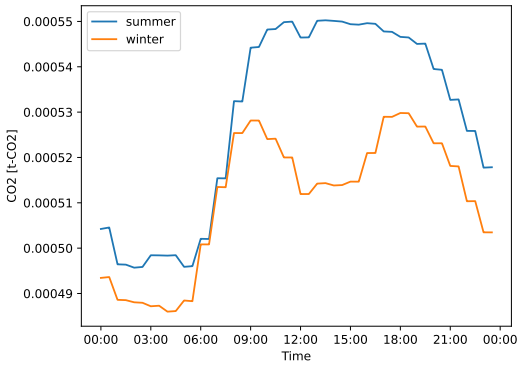

Figure 4: CO_2 emission coefficient movement in the summer and winter (averaged of 100 simulations)

4.1 Peak-Cut

4.1.1 Fixed Cut Scenario

This scenario employs peak-cut DR at fixed time periods for the entire factory. The factory cuts the demand in the ratio r during the daytime (12:00 – 15:00) in the summer and evening (17:00 – 20:00) in the winter; these are periods during which the market power price is comparatively high. This demand-cut ratio r is crucial for industrial production. Thus, we limit it to 0.2. Accordingly, we test four patterns of r: $[0.05, 0.1, 0.15, 0.2]$.

4.1.2 Flexible Cut Scenario

This scenario differs slightly from the fixed cut scenario in terms of the selection of time periods. In the flexible cut scenario, the time periods for DR actions are selected based on the indices, such as price, CO_2 emission, and demand of the same market in the previous week. Based on these criteria, six markets (30-minute periods $\times 6 = 3.0$ h) are selected in the working hours 9:00 – 17:00.

4.2 Peak Shift

4.2.1 AC Shift Scenario (Summer Only)

This scenario only controls the AC, and aims to reduce the peak demand and increase usage at other times instead. By employing a peak shift instead of a peak cut, we can avoid a significant decrease in the level of room comfort. In this scenario, the periods of demand reduction are determined based on the top three hours with the highest air conditioning usage in the actual summer data and set to 14:00 – 17:00. Meanwhile, the demand is increased between 9:00 – 14:00. We also set the DR ratio, r, to $[0.25, 0.5, 0.75, 1.0]$. For example, if $r = 1$, the AC is stopped completely during 14:00 – 17:00. Meanwhile, during 9:00 – 14:00, the power shaved off during the demand is allocated uniformly and used. This scenario can only be used in summer.

4.2.2 Work Time Shift Scenario

The work time shift scenario aims to shift the factory's working hours ahead to reduce the peak load as the morning demand is smaller than evening demand. We change the ratio of the target DR, $r \in [0.25, 0.5, 0.75, 1.0]$, and the number of hours by which the factory's usual working hours are shifted, $m \in [0.5, 1.0, 1.5, 2.0, 2.5, 3.0]$. For example, if $r = 1.0$ and $m = 3.0$, the working hours of the factory are set to 6:00 – 14:00. Similarly, if $r = 0.5$ and $m = 0.5$, only half of the factory is working from 8:30 am, whereas the others remain the same as the usual working hours (9:00 – 17:00).

4.2.3 Fixed Shift Scenario

This scenario controls the total demand of the factory to reduce peak demand and increase its usage at other times instead. The downward DR (demand reduction) and upward DR (demand increase) periods are predefined in the fixed shift scenario. In the summer, downward DR is active during 12:00 – 15:00, while upward DR is active during 9:00 – 12:00 and 15:00 – 17:00. However, in the winter, downward DR is active during 9:00 – 10:30 and 15:30 – 17:00, while upward DR is active during 10:30 – 15:30. In the downward DR periods, the demand ratio r is reduced and the demand is distributed equally in the upward DR periods.

4.2.4 Flexible Shift Scenario

This scenario differs slightly from the fixed shift scenario in terms of the selection of time periods. In the flexible shift scenario, the time periods for upward and downward DR activation are selected based on the indices for price, CO_2 emission, and demand of the same market in the previous week. Based on these criteria, each of the six markets (30-minute

periods $\times 6 = 3.0$ h) during the working hours (9:00 – 17:00) for upward and downward DR are selected.

5 Experiments

First, we tuned the undetermined hyperparameters based on the criterion that the mean and standard deviation of the prices as close to the real data of the JEPX. Consequently, $W_C^g = 10.0, W_N^g = 12.5, W_C^d = 1.0$, and $W_N^d = 12.5$.

The tuned hyperparameters were used to analyze each DR scenario. For each scenario, 100 simulations were performed (one simulation = one year). Next, the effectiveness of each DR scenario was analyzed and compared to the baseline scenario with no DR.

Finally, two evaluation indicators were employed to check the effectiveness of each DR. First, a cost reduction efficiency indicator that indicates how efficiently the DR scenario reduced costs. Second, a CO_2 emission reduction efficiency indicator, which represents how efficiently the DR scenario reduced CO_2 emissions. These indicators are respectively defined as follows:

$$E_{\text{cost}} = \frac{R_{\text{cost}}}{R_{\text{demand}}} + \varepsilon, \tag{14}$$

$$E_{\text{CO}_2} = \frac{R_{\text{CO}_2}}{R_{\text{demand}}} + \varepsilon, \tag{15}$$

$$\varepsilon = \begin{cases} 0 & \text{(Peak Cut)} \\ 1 & \text{(Peak Shift)} \end{cases} \tag{16}$$

$$R_{\text{demand}} = \frac{\sum_t \sum_k \max(\overline{d}_t^k - d_t^k, 0)}{\sum_t \sum_k \overline{d}_t^k}, \tag{17}$$

$$R_{\text{cost}} = \frac{\sum_t \sum_k (\overline{p}_t^k \overline{d}_t^k - p_t^k d_t^k)}{\sum_t \sum_k \overline{p}_t^k \overline{d}_t^k}, \tag{18}$$

$$R_{\text{CO}_2} = \frac{\sum_t \sum_k (\overline{e}_t^k \overline{d}_t^k - e_t^k d_t^k)}{\sum_t \sum_k \overline{e}_t^k \overline{d}_t^k}, \tag{19}$$

where p_t^k, d_t^k, and e_t^k are the price, demand, and CO_2 emission coefficient in the kth market on day t ($t \in [60, 61, \cdots, 152]$ in the summer and $t \in [244, 245, \cdots, 334]$ in the winter), respectively, whereas $\overline{p}_t^k, \overline{d}_t^k$, and $\overline{e}_t^k$ are those in the baseline scenario. E_{cost} and E_{CO_2} are the cost reduction efficiency and CO_2 emission reduction efficiency metrics, respectively. $R_{\text{demand}}, R_{\text{cost}}$, and R_{CO_2} are the ratios of demand control, cost reduction, and CO_2 emissions reduction, respectively. Notably, the demand control ratio is calculated only by downward DR. Thus, E_{cost} and E_{CO_2} imply the cost reduction ratio per demand control ratio and CO_2 emission reduction ratio per demand control ratio, respectively. However, these metrics differ between the peak shifts and peak-cut scenarios. In the case of peak-cut, the ratios of demand reduction and that of cost reduction are almost the same if we assume that factory production is scaled in a homothetic manner. In contrast, in the case of peak shift, the total factory production is assumed to be almost the same. These relationships can also be applied to CO_2 emissions. Thus, we employ the coefficient adjustment term ε as mentioned above. Note that E_{cost} and E_{CO_2} are nondimensional numbers. Thus, these evaluation indicators do not depend on DR scales, such as r for each DR scenario. This enables us to evaluate all DR scenarios at the same scale.

6 Results

6.1 Each DR Scenario

6.1.1 *Fixed Cut Scenario*

Figures 5 and 6 show the results for the fixed cut scenario. As mentioned above, in the summer, DR is activated only during the daytime, while in the winter, it is activated only in the evening. Figure 5 shows the demand reduction ratio and CO_2 emission reduction ratio. Depending on the season, both are linearly scaled based on the DR ratio r. According to this graph, a larger DR is achieved in the summer. However, the ratio of demand reduction and CO_2 emission reduction is almost the same for all data points. If it is the same or below, CO_2 emission reduction can only be achieved by demand reduction. To investigate whether the reductions in CO_2 emissions and costs are beyond the direct effects of demand reduction, the two aforementioned evaluation indicators are plotted in Figure 6. Because the horizontal axis is the demand reduction ratio, the points in each series are arranged from left to right in the ascending order of the DR scale r. The results reveal that the daytime DR in the summer is slightly better than the evening DR in winter in terms of reduction efficiency. Nevertheless, the efficiency factor is statistically greater than 1 in both summer and winter, suggesting that this DR scenario is still working correctly.

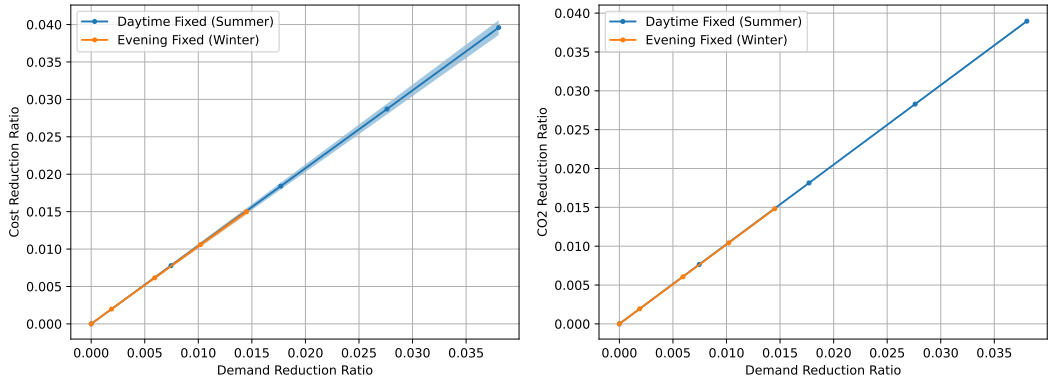

Figure 5: Cost (left) and CO_2 emission (right) reduction ratios for each demand reduction ratio in the fixed cut scenario. The filled areas are the 95% confidential intervals (CI). The filled areas in the right figure are too small to be seen in the figure.

6.1.2 *Flexible Cut Scenario*

Figures 7 and 8 show the results for the flexible cut scenario. Figure 7 indicates that the flexible cut scenario shows the linear response of CO_2 emission and cost reductions to demand reduction. Figure 8 enables us to conduct a more precise analysis of the efficiencies. The efficiencies of all scenarios with the three market selection criteria are statistically above 1 in both summer and winter, suggesting that this DR scenario is also working correctly. Although not statistically significant, price-based market selection DR shows the best cost reduction efficiency. In contrast, CO_2- and demand-based market selection DRs show almost similarly high CO_2 emissions reduction efficiency.

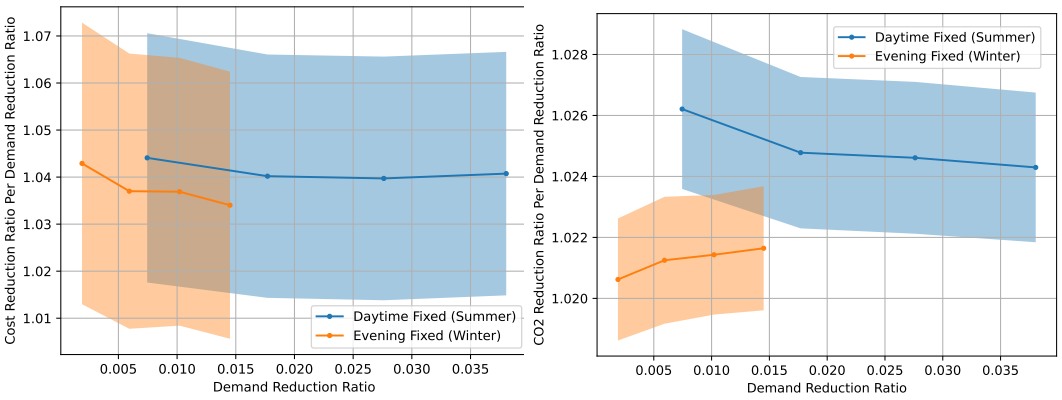

Figure 6: Cost (left) and CO_2 emission (right) reduction efficiencies in the fixed cut scenario. The filled areas are 95% CI.

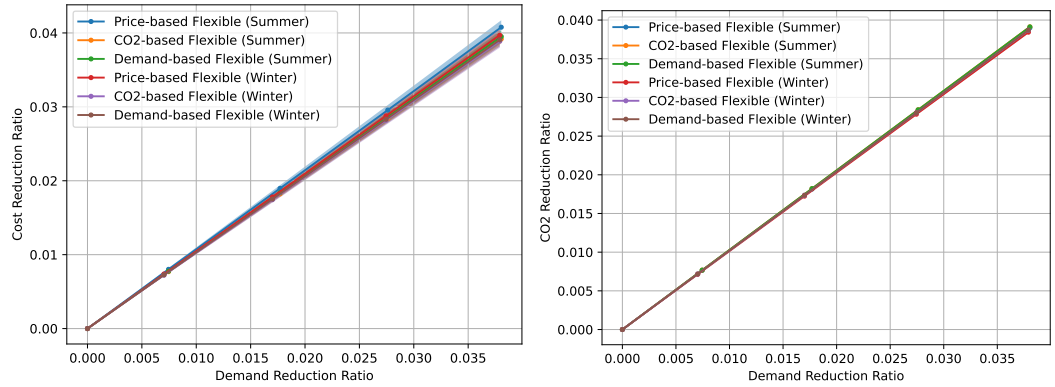

Figure 7: Cost (left) and CO_2 emissions (right) reduction ratios for each demand reduction ratio in the flexible cut scenario. The filled areas are the 95% CI.

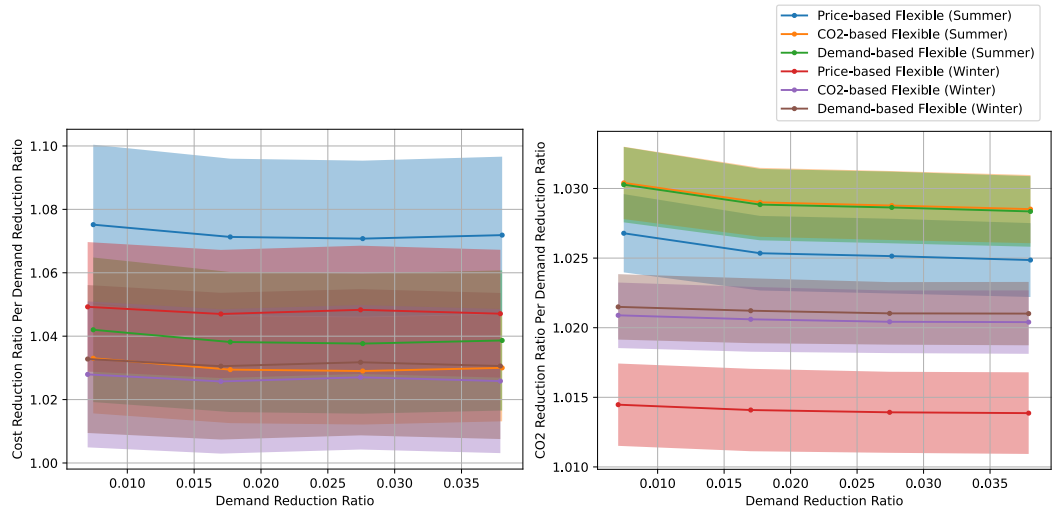

Figure 8: Cost (left) and CO_2 emissions (right) reduction efficiencies in the flexible cut scenario. The filled areas are the 95% CI.

6.1.3 AC Shift Scenario (Summer Only)

Figures 9 and 10 show the results of the AC shift scenario. First, Figure 9 shows the relationship between the cost or CO_2 emissions reductions, and the demand shift. These reductions show a linear response on average to the demand shift with positive coefficients. However, the variance compared with the mean is significant. Figure 10 provides a more detailed analysis of the efficiencies. Note that in Figure 10, in contrast to the peak-cut scenarios, the vertical axis is $(E_{\text{cost}} - 1)$ and $(E_{\text{CO}_2} - 1)$ instead of E_{cost} and E_{CO_2}, respectively. This is common among all results of the peak shift scenarios. We find that although the cost reduction efficiency is not statistically significant, this DR scenario may barely work in terms of both the cost and CO_2 emissions reduction.

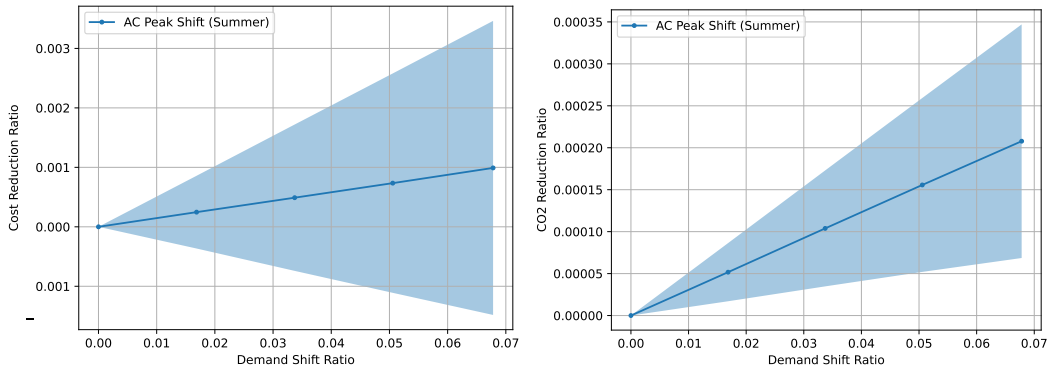

Figure 9: Cost (left) and CO_2 emissions (right) reduction ratios for each demand reduction ratio in the AC shift scenario. The filled areas are the 95% CI.

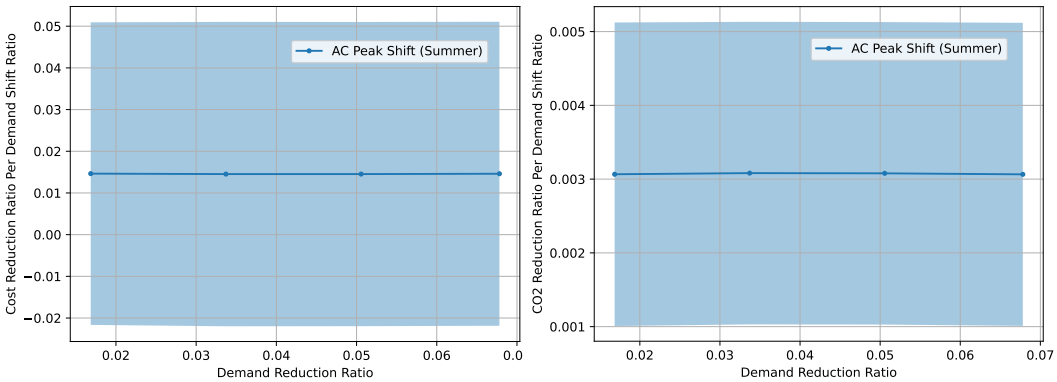

Figure 10: Cost (left) and CO_2 emissions (right) reduction efficiencies in the AC shift scenario. The filled areas are the 95% CI. We use $(E_{\text{cost}} - 1)$ and $(E_{\text{CO}_2} - 1)$ instead of E_{cost} and E_{CO_2}, respectively.

6.1.4 Work Time Shift Scenario

Figures 11 and 12 show the results of the work time shift scenario. Interestingly, the performance in winter is mostly negative. This implies that in the winter, the morning price and CO_2 emission coefficients are higher than those in the evening, and the DR is counterproductive. However, the summer performance is large, with longer work time shifts

producing larger DR effects. According to Figure 11, cost and CO_2 emissions reductions almost always have linear responses to the demand shift. However, the coefficients differ depending on the setting and are shown in Figure 12.

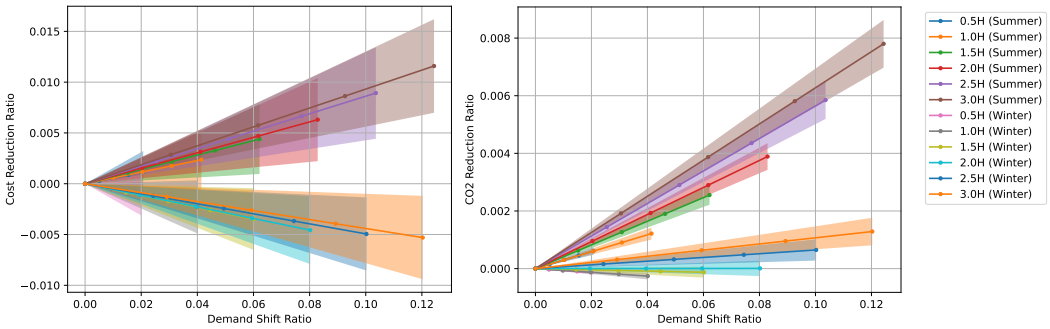

Figure 11: Cost (left) and CO_2 emissions (right) reduction ratios for each demand reduction ratio in the work time shift scenario. The filled areas are the 95% CI.

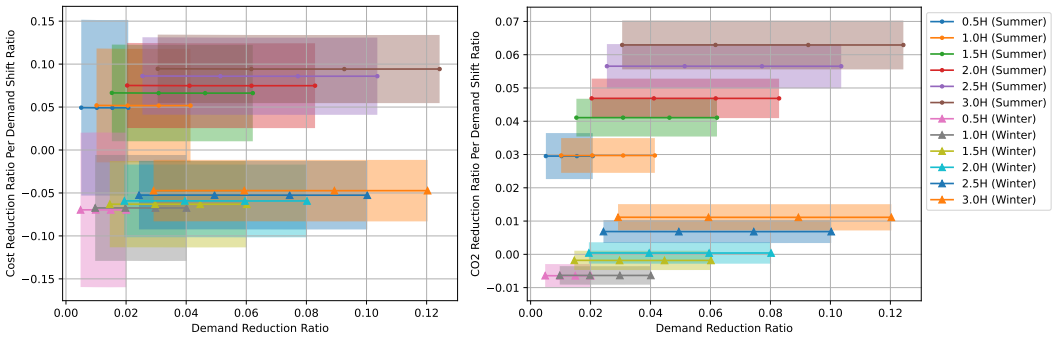

Figure 12: Cost (left) and CO_2 emissions (right) reduction efficiencies in the work time shift scenario. The filled areas are the 95% CI. We use $(E_{\text{cost}} - 1)$ and $(E_{CO_2} - 1)$ instead of E_{cost} and E_{CO_2}, respectively.

6.1.5 Fixed Shift Scenario

Figures 13 and 14 show the results for the fixed shift scenario. Figure 13 shows that the cost reduction performance is almost same between summer and winter. By contrast , the CO_2 emissions reductions are completely different. This tendency is also observed in Figure 14. Although the cost reduction efficiency is not statistically significant, the CO_2 emissions reduction efficiency in the winter is significant. In contrast, the CO_2 emissions reduction efficiency in the summer is almost 0. These results suggest that the fixed DR periods need to be correctly selected to maximize the DR effect because this difference comes from the price and CO_2 emission coefficient of electricity during the peak shift periods.

6.1.6 Flexible Shift Scenario

Figures 15 and 16 show the results for the flexible-shift scenario. Figure 15 shows that the fluctuation in the results is significantly high. Moreover, in some settings, the cost and

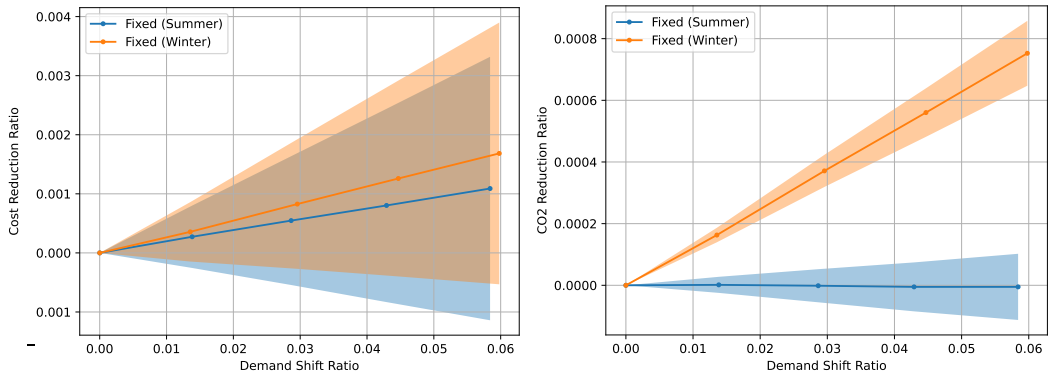

Figure 13: Cost (left) and CO_2 emissions (right) reduction ratios for each demand reduction ratio in the fixed shift scenario. The filled areas are the 95% CI.

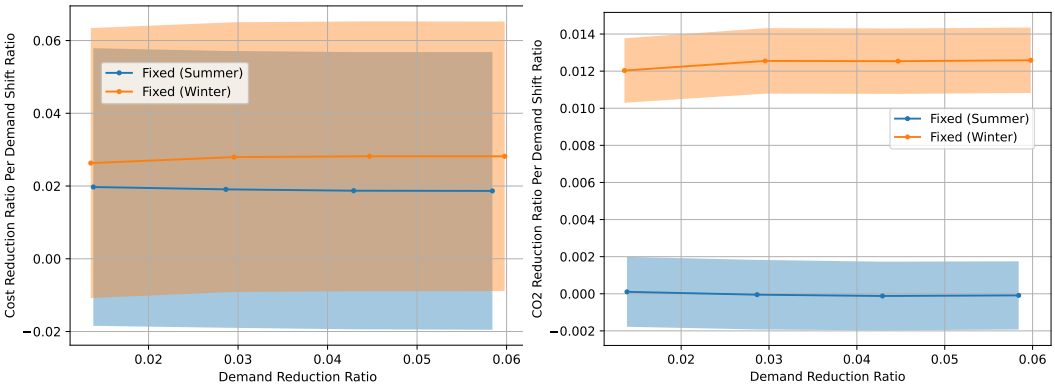

Figure 14: Cost (left) and CO_2 emissions (right) reduction efficiencies in the fixed shift scenario. The filled areas are the 95% CI. We use $(E_{\text{cost}} - 1)$ and $(E_{CO_2} - 1)$ instead of E_{cost} and E_{CO_2}, respectively.

CO_2 emissions reduction ratios are not statistically significant, even when the demand shift ratio is high. Figure 16 shows that the price-based market selection DR exhibits the best cost reduction efficiency in summer and winter. However, the CO_2- and demand-based DRs show almost similarly high CO_2 emissions reduction efficiency. Moreover, although the cost reduction efficiencies in summer and winter are almost similar, the CO_2 emissions reduction efficiency in winter is significantly higher than that in summer.

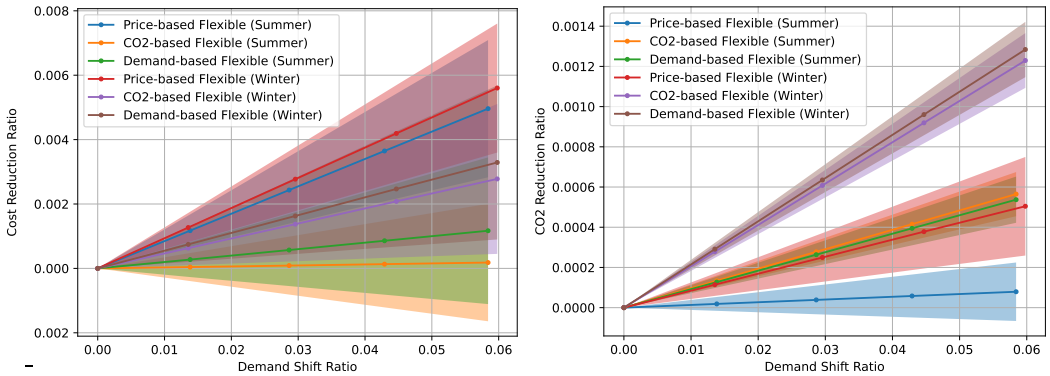

Figure 15: Cost (left) and CO_2 emissions (right) reduction ratios for each demand reduction ratio in the flexible shift scenario. The filled areas are the 95% CI.

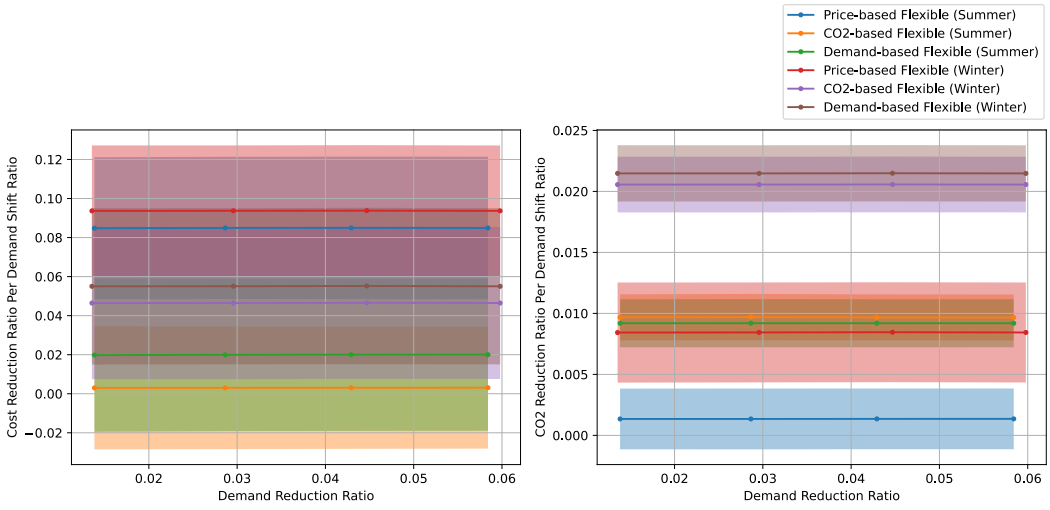

Figure 16: Cost (left) and CO_2 emissions(right) reduction efficiencies in the flexible shift scenario. The filled areas are the 95% CI. We use $(E_{\text{cost}} - 1)$ and $(E_{\text{CO}_2} - 1)$ instead of E_{cost} and E_{CO_2}, respectively.

6.2 Comparison between DR Scenarios

Figures 17 and 18 show the comparisons of all scenarios in both summer and winter in terms of cost and CO_2 emissions reduction efficiencies, respectively. As explained in Section 5, between the peak-cut and peak shift scenarios, the efficiency indicators are converted using ε defined in Eq. 16. In these figures, the parts of the bars corresponding to ε are indicated

by dotted lines. Moreover, only the results from the largest DR scale for each scenario are used in the figures. This is because according to the Figures 5, 7, 9, 11, 13, and 15, the responses of cost and CO_2 emissions to the demand cut/shift ratio are almost always linear.

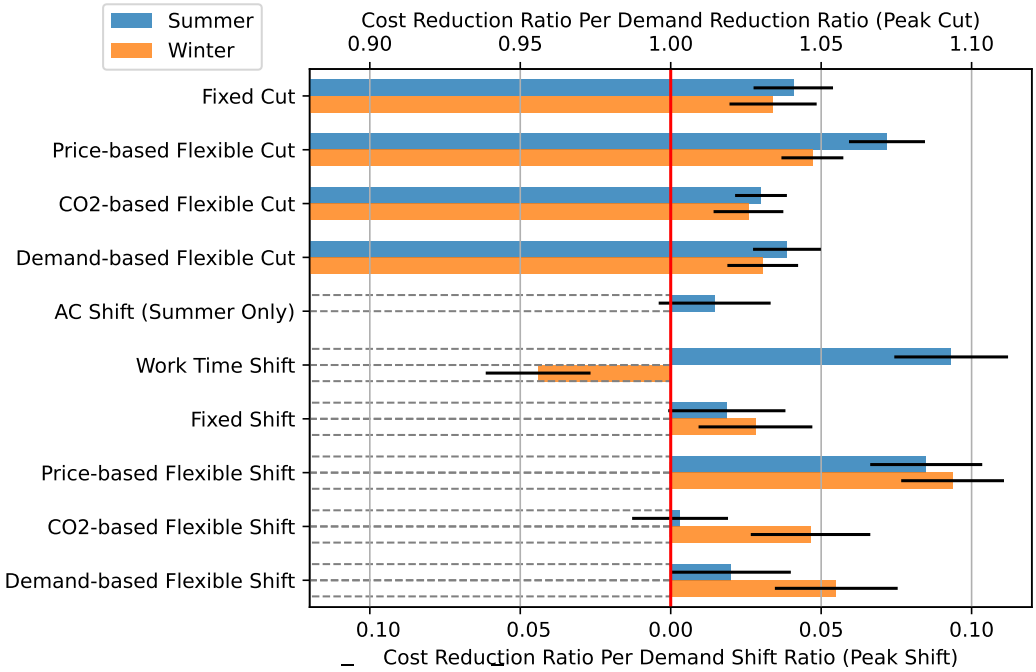

Figure 17: Cost reduction efficiency comparison of all scenarios. The error bars are standard deviation.

The red lines in the figures represent the borderline where the reduction in production activities due to DR exceeds the effects of DR. This shows that only the work time shift scenario in winter falls below the borderline for cost reduction efficiency. In terms of CO_2 emissions reduction efficiency, all scenarios exceed the borderline. Although not statistically significant, the work time shift in winter and price-based flexible shift in both summer and winter show relatively high cost reduction efficiencies despite their high variability. Conversely, in terms of CO_2 emissions reduction efficiency, only the work time shift scenario in summer shows statistically highest results.

7 Discussion

First, we discuss the peak-cut scenarios. In the fixed cut scenario, the effect of DR during winter was relatively small. This was probably because the period when DR was activated under this scenario was outside the factory's working hours and the absolute scale of DR was small. However, the indices-based flexible peak-cuts appeared to be effective. Interestingly, the demand-based flexible peak-cut performed well in terms of CO_2 emissions reduction efficiency. This may be because the CO_2 emission factor is relatively high when demand is high owing to the high utilization of thermal power plants. In the peak-cut scenario, the effect of the DR scenarios is larger because the plants need to stop. Therefore, if peak-cut DR is adopted, it is necessary to achieve sufficient benefits, such as sufficient CO_2 emissions reduction. It is also practically difficult to repeatedly trigger a 30-minute DR at

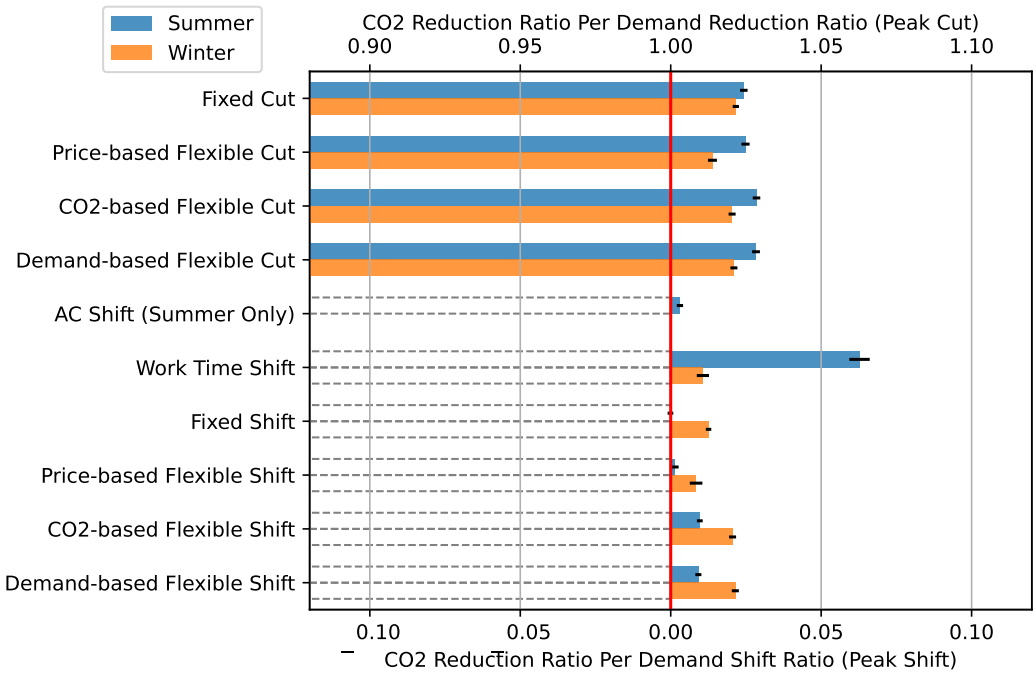

Figure 18: CO_2 emissions reduction efficiency comparison of all scenarios. The error bars are standard deviation.

different times. Therefore, adopting a fixed peak-cut scenario with consecutive DR periods may be more practically beneficial than adopting a flexible peak-cut scenario.

Second, we obtained interesting results regarding the peak shift scenarios. The AC shift scenario showed no CO_2 emissions reduction effect and a limited cost reduction effect. This suggests that the AC shift scenario may be inappropriate due to the tradeoff for room comfort. However, the work time shift scenario had significant cost and CO_2 emission reductions in the summer. This is perhaps because the price and CO_2 emission coefficient were lower in the early morning than in the evening. In winter, this tendency does not appear; thus, the performance in winter is not similar. For the fixed and flexible shift scenarios, as in the peak-cut scenarios, the performance of the winter fixed shift scenario was low, whereas the CO_2 emissions reduction performance was high in the CO_2- and demand-based flexible shift scenarios.

Comparing all scenarios, the work time shift scenario showed the best results for both the cost and CO_2 emission reduction efficiencies. The peak shift scenario is the preferred scenario because it reduces both costs and CO_2 emissions efficiently with no change in overall factory production. Moreover, the work time shift scenario is more efficient because it can be achieved by changing the factory's operating hours. Thus, the work time shift scenario does not require shutting down the factory during the working hours. Conversely, the work time shift scenario in winter does not work well because a good match between factory working hours, and the winter price and CO_2 emission factor curves does not emerge. The work time shift does not work well in the winter, whereas the flexible shift scenario is moderately efficient in winter. Meanwhile, the flexible shift scenario can achieve better efficiency by selecting the appropriate indicators for the DR period.

Our work can also be advanced in some areas. Currently, carbon-neutral power sources

and their availability are limited. Hence, achieving even small CO_2 emissions reductions, such as those by DR, is important. Although multi-agent simulations can provide insightful results, our current multi-agent simulation needs to be updated. For example, on-site generation (solar photovoltaic or wind power generation), batteries, and fuel cells have recently shown promise as decarbonization solutions. Thus, by adding these features along with factory agents, we can create simulations that can better evaluate the various DR scenarios. Another strength of multi-agent simulation is its ability to analyze fictional scenarios in fictional factories, even where actual data may not exist. It can analyze the impact of oil price increases and other changes in the external environment on DR strategies, which can helpful in dealing with the unstable social conditions of recent years.

Multi-agent simulation is a powerful tool for analyzing the details of social phenomena such as decarbonization. In this study, the factory size was limited. However, we can realize the market impacts in our simulation even if the factory has a significant effect on the market. In addition, although only the previous-day spot market is used here because of its large market share, more realistic procurement strategies can be considered by modeling other markets. Finally, one can investigate various decarbonization strategies by modeling the CO_2 emissions trading market.

8 Conclusion

We constructed a multi-agent simulation of the electric power market and analyzed several DR scenarios. The simulation model was constructed based on actual data from the Japanese market and a factory. We simulated changes in the factory's electricity consumption behavior under various DR scenarios, and evaluated the cost and CO_2 emission reduction efficiencies, which were newly defined in this study. The results showed that shifting the working hours of the factory ahead during the summer was effective. Conversely, peak shift during the winter was effective. Thus, we demonstrated the usefulness of our multi-agent simulation for examining the effects of complex DR scenarios by considering seasonal and time-of-day electric power characteristics. Future work should address the validity of our analysis by applying each DR scenario in the actual market. In addition, more complex and realistic decarbonization strategies can be simulated by adding decarbonization methods such as on-site power generation, batteries, and fuel cells.

References

[1] P. L. Joskow, "Introduction to electricity sector liberalization: lessons learned from cross-country studies," *Electricity market reform: an international perspective*, vol. 1, pp. 1–32, 2006.

[2] K. Hohki, "Outline of Japan Electric Power Exchange (JEPX)," *IEEJ Transactions on Power and Energy*, vol. 125, no. 10, pp. 922–925, 2005.

[3] V. Masson-Delmotte, P. Zhai, H.-O. Pörtner, D. Roberts, J. Skea, P. R. Shukla, A. Pirani, W. Moufouma-Okia, C. Péan, R. Pidcock *et al.*, "An IPCC Special Report on the impacts of global warming of Global warming of 1.5 °C," 2018.

[4] M. H. Albadi and E. F. El-Saadany, "A summary of demand response in electricity markets," *Electric Power Systems Research*, vol. 78, no. 11, pp. 1989–1996, 2008.

[5] A. Helleboogh, G. Vizzari, A. Uhrmacher, and F. Michel, "Modeling dynamic environments in multi-agent simulation," *Autonomous Agents and Multi-Agent Systems*, vol. 14, no. 1, pp. 87–116, 2007.

[6] H. Kitano and S. Tadokoro, "RoboCup Rescue: A Grand Challenge for Multiagent and Intelligent Systems," *AI Magazine*, vol. 22, no. 1, pp. 39–39, 2001.

[7] P. Trigo and P. Marques, "The electricity market as a multi-agent system," in *Proceedings of the 5th International Conference on the European Electricity Market*. IEEE, 2008, pp. 1–6.

[8] F. Sensfuß, "Assessment of the impact of renewable electricity generation on the German electricity sector: An agent-based simulation approach," 2007, https://doi.org/10.5445/IR/100000777.

[9] F. Sensfuß, M. Ragwitz, and M. Genoese, "The merit-order effect: A detailed analysis of the price effect of renewable electricity generation on spot market prices in Germany," *Energy Policy*, vol. 36, no. 8, pp. 3086–3094, 2008.

[10] O. Weiss, D. Bogdanov, K. Salovaara, and S. Honkapuro, "Market designs for a 100% renewable energy system: Case isolated power system of Israel," *Energy*, vol. 119, pp. 266–277, 2017.

[11] S. Kan and Y. Shibata, "Study on FIP Policy Design by Using Multi-agent Based Electric Power Market Simulation Model," 2020, https://eneken.ieej.or.jp/en/report_detail.php?article_info_id=8918.

[12] A. S. Chuang, F. Wu, and P. Varaiya, "A game-theoretic model for generation expansion planning: Problem formulation and numerical comparisons," *IEEE Transactions on Power Systems*, vol. 16, no. 4, pp. 885–891, 2001.

[13] C. J. Day and D. W. Bunn, "Divestiture of Generation Assets in the Electricity Pool of England and Wales: A Computational Approach to Analyzing Market Power," *Journal of Regulatory Economics*, vol. 19, no. 2, pp. 123–141, 2001.

[14] Y. Jiang, K. Zhou, X. Lu, and S. Yang, "Electricity trading pricing among prosumers with game theory-based model in energy blockchain environment," *Applied Energy*, vol. 271, p. 115239, 2020.

[15] M. Ghaffari, A. Hafezalkotob, and A. Makui, "Analysis of implementation of Tradable Green Certificates system in a competitive electricity market: A game theory approach," *Journal of Industrial Engineering International*, vol. 12, no. 2, pp. 185–197, 2016.

[16] J. K. Kok, C. J. Warmer, and I. G. Kamphuis, "PowerMatcher: multiagent control in the electricity infrastructure," in *Proceedings of the fourth international joint conference on Autonomous agents and multiagent systems*, 2005, pp. 75–86.

[17] H. S. Oh and R. J. Thomas, "Demand-side bidding agents: Modeling and simulation," *IEEE Transactions on Power Systems*, vol. 23, no. 3, pp. 1050–1056, 2008.

[18] Z. Zhou, F. Zhao, and J. Wang, "Agent-based electricity market simulation with demand response from commercial buildings," *IEEE Transactions on Smart Grid*, vol. 2, no. 4, pp. 580–588, 2011.

[19] T. Torii, K. Izumi, and K. Yamada, "Shock transfer by arbitrage trading: analysis using multi-asset artificial market," *Evolutionary and Institutional Economics Review*, vol. 12, no. 2, pp. 395–412, 2015.